

PoS(LATTICE2024)323

ADP-25-2/T1264

DESY-25-011

Liverpool LTH 1391

Renormalisation Group Equations for 2+1 clover fermions

**K. U. Can,^a R. Horsley,^{b,1,*} P. E. L. Rakow,^c G. Schierholz,^d H. Stüben,^e
R. D. Young^a and J. M. Zanotti^a**

^a*CSSM, Department of Physics, University of Adelaide, Adelaide SA 5005, Australia*

^b*School of Physics and Astronomy, University of Edinburgh, Edinburgh EH9 3FD, UK*

^c*Theoretical Physics Division, Department of Mathematical Sciences, University of Liverpool,
Liverpool L69 3BX, UK*

^d*Deutsches Elektronen-Synchrotron DESY, Notkestr. 85, 22607 Hamburg, Germany*

^e*Universität Hamburg, Regionales Rechenzentrum, 20146 Hamburg, Germany*

E-mail: rhorsley@ph.ed.ac.uk

Many lattice QCD simulations now have many lattice spacings available, and it is of interest to investigate how they scale. In this talk we first derive renormalisation group equations appropriate for 2+1 clover fermions. This is then used together with pion mass and gradient flow results at five lattice spacings to study scaling.

*The 41st International Symposium on Lattice Field Theory (LATTICE2024)
28 July - 3 August 2024
Liverpool, UK*

¹For the QCDSF Collaboration

*Speaker

1. Introduction

One of the major difficulties in lattice gauge theories is the extrapolation to the continuum limit. Usually individual fits at a particular lattice spacing are made to, e.g. a hadron mass or matrix element, followed by an extrapolation to the continuum limit (usually in a^2). This is a noisy procedure, involving both the pre-determined a values and also the individual values of the mass or matrix element. To improve the situation often a smoothing procedure is used, for example a joint extrapolation involving both the lattice spacing and mass or matrix element simultaneously. Theoretically this is often not so well justified. A better motivated procedure suggested here is to use the Renormalisation Group (RG) equations to help to achieve this. In this contribution we attempt a first step by deriving and solving the RG equations for the lattice spacing.

2. The RG equation

Scaling means that we have lines of constant physics (e.g. constant mass ratios) passing through our parameter space. On one of these lines we can measure the relative rate at which lattice spacing changes by monitoring the rate at which correlation lengths change as we move along the trajectory. Scaling (up to $O(a^2)$ violations) are regions where $a\Lambda^{\text{lat}} \ll 1$ and $am_q \ll 1$. For Wilson type fermions considered here we have in g_0, κ_q space

$$a \frac{\partial}{\partial a} \Big|_{\text{physics}} = U(g_0, \{\kappa\}) \frac{\partial}{\partial g_0} \Big|_{\kappa} + \sum_q V_q(g_0, \{\kappa\}) \frac{\partial}{\partial \kappa_q} \Big|_{g_0}. \quad (1)$$

Re-writing this in terms of $m_q^{\text{lat}} \equiv am_q$ where

$$am_q \equiv \frac{1}{2} \left(\frac{1}{\kappa_q} - \frac{1}{\kappa_{0c}(g_0)} \right), \quad (2)$$

(with κ_0 the hopping parameter on the $SU(n_f)$ -flavour symmetric line, with critical point at the chiral limit κ_{0c}) and then Taylor expanding U and V_q gives

$$\begin{aligned} a \frac{\partial}{\partial a} \Big|_{\text{physics}} &= B_0(g_0) \frac{\partial}{\partial g_0} \Big|_{\{am\}} + B_1(g_0) a \bar{m} \frac{\partial}{\partial g_0} \Big|_{\{am\}} \\ &+ G_0(g_0) \sum_q am_q \frac{\partial}{\partial am_q} \Big|_{g_0} + H_0(g_0) a \bar{m} \sum_q \frac{\partial}{\partial am_q} \Big|_{g_0} \\ &+ G_1(g_0) a \bar{m} \sum_q am_q \frac{\partial}{\partial am_q} \Big|_{g_0} + G_2(g_0) \sum_q (am_q)^2 \frac{\partial}{\partial am_q} \Big|_{g_0} \\ &+ H_1(g_0) (a \bar{m})^2 \sum_q \frac{\partial}{\partial am_q} \Big|_{g_0} + H_2(g_0) a^2 \bar{m}^2 \sum_q \frac{\partial}{\partial am_q} \Big|_{g_0}, \end{aligned} \quad (3)$$

where

$$a \bar{m} \equiv \frac{1}{n_f} \sum_q am_q, \quad a^2 \bar{m}^2 \equiv \frac{1}{n_f} \sum_q a^2 m_q^2. \quad (4)$$

The B_0, G_0, H_0 coefficients are usually referred to as ‘renormalisation’, while the B_1, G_1, G_2, H_1, H_2 coefficients are the ‘improvement’ terms, so in principle this treats both the renormalisation and

improvement terms in a unified fashion. For chiral fermions all the coefficients vanish, except for B_0 and G_0 .

It is sufficient to only consider here the leading terms (ie $O(am_q)$), although the higher order terms can be considered, [1]. The leading functions are related to the usual renormalisation coefficients

$$B_0(g_0) = -\beta(g_0), \quad G_0(g_0) = 1 - \gamma_m^{\text{NS}}(g_0), \quad H_0(g_0) = \gamma_m^{\text{NS}}(g_0) - \gamma_m^{\text{S}}(g_0), \quad (5)$$

with

$$\begin{aligned} \beta(g_0) &= -b_0 g_0^3 - b_1 g_0^5 - b_2^{\text{lat}} g_0^7 + O(g_0^9), & \gamma_m^{\text{NS}}(g_0) &= d_0 g_0^2 + d_1^{\text{NS lat}} g_0^4 + O(g_0^6), \\ B_1(g_0) &= b_{10}^{\text{lat}} g_0^3 + O(g_0^5), & \gamma_m^{\text{S}}(g_0) &= d_0 g_0^2 + d_1^{\text{S lat}} g_0^4 + O(g_0^6), \end{aligned} \quad (6)$$

where b_0 , b_1 and d_0 are known universal coefficients.

2.1 Renormalised quark masses

For Wilson-like fermions, which have no chiral symmetry, the singlet and non-singlet quark mass pieces evolve differently

$$\bar{m}^{\text{rgi}} = a\bar{m} u(g_0), \quad m_q^{\text{rgi}} - \bar{m}^{\text{rgi}} = (am_q - a\bar{m}) v(g_0). \quad (7)$$

For simplicity we consider the Renormalised Group Invariant (RGI) quark mass, alternatively the same equations hold for the quark mass in a given scheme at a given scale. Also to simplify the notation somewhat we have absorbed Λ^{lat} into the definition of \bar{m}^{rgi} , i.e. we measure the quark mass in units of Λ^{lat} . Note, in particular, that $\bar{m}^{\text{rgi}} \propto a\bar{m}$.

We now solve the RG equation

$$a \left. \frac{\partial}{\partial a} \right|_{\text{physics}} m_q^{\text{rgi}} = 0, \quad (8)$$

to give

$$u(g_0) = C(g_0) \exp \left[\int_0^{g_0} d\xi \left\{ \frac{1}{b_0 \xi^3} - \frac{b_1 + b_0 d_0}{b_0^2 \xi} - \frac{G_0(\xi) + H_0(\xi)}{B_0(\xi)} \right\} \right], \quad (9)$$

and

$$v(g_0) = C(g_0) \exp \left[\int_0^{g_0} d\xi \left\{ \frac{1}{b_0 \xi^3} - \frac{b_1 + b_0 d_0}{b_0^2 \xi} - \frac{G_0(\xi)}{B_0(\xi)} \right\} \right], \quad (10)$$

where

$$C(g_0) = \Lambda^{\text{lat}} [2b_0 g_0^2]^{\frac{d_0}{2b_0}} [b_0 g_0^2]^{\frac{b_1}{2b_0^2}} \exp \left[\frac{1}{2b_0 g_0^2} \right]. \quad (11)$$

These are the usual type of equations, arranged so that there is no singularity in the integral as $g_0 \rightarrow 0$. Again, for simplicity, as for \bar{m}^{rgi} we shall in future measure u (and v) in units of Λ^{lat} , so $u \rightarrow u/\Lambda^{\text{lat}}$. Similar equations (with appropriate γ s) also hold for the renormalisation of operators $m^{\text{rgi}} \rightarrow O^{\text{rgi}}$. However we shall not consider this further here.

2.2 Coupling constant

Rather than considering the renormalised coupling, we consider here the relation between the lattice spacing and lattice coupling. There are two possibilities. First we consider changing lattice spacing (i.e. including $a\bar{m}$ in the definition, but keeping the coupling constant). Setting

$$a = s(g_0) \{1 + a\bar{m} r(g_0)\} , \quad (12)$$

and solving

$$a \left. \frac{\partial}{\partial a} \right|_{\text{physics}} a = a , \quad (13)$$

gives

$$s(g_0) = A(g_0) \exp \left(\int_0^{g_0} d\xi \left\{ \frac{1}{B_0(\xi)} - \frac{1}{b_0 \xi^3} + \frac{b_1}{b_0^2 \xi} \right\} \right) , \quad (14)$$

$$r(g_0) = -u(g_0) \int_0^{g_0} d\xi \frac{B_1(\xi)}{u(\xi) B_0^2(\xi)} \underbrace{=}_{g_0^2 \rightarrow 0} -\frac{b_{10}^{\text{lat}}}{b_0} g_0^2 + O(g_0^4) , \quad (15)$$

with

$$A(g_0) = \frac{1}{\Lambda^{\text{lat}}} [b_0 g_0^2]^{-\frac{b_1}{2b_0^2}} \exp \left[-\frac{1}{2b_0 g_0^2} \right] . \quad (16)$$

Note that $s(g_0)$ is the standard RG solution to the β -function. Alternatively a second possibility would be to re-define the coupling constant by setting (e.g. [2])

$$\tilde{g}_0^2 = g_0^2 \{1 + b_g(g_0) a\bar{m}\} , \quad (17)$$

and now solving

$$a \left. \frac{\partial}{\partial a} \right|_{\text{physics}} \tilde{g}_0 = B_0(\tilde{g}_0) , \quad (18)$$

gives

$$b_g(g_0) = 2 \frac{B_0(g_0)}{g_0} r(g_0) \underbrace{=}_{g_0^2 \rightarrow 0} -2b_{10}^{\text{lat}} g_0^4 + O(g_0^6) . \quad (19)$$

As anticipated we have $b_g \propto r$. As discussed in e.g. [3, 4] we expect b_g (and hence r) to be numerically quite small.

3. Lattice data

For $n_f = 2 + 1$, $q = u, d, s$ flavours ($am_u = am_d \equiv am_l$) the QCDSF strategy [5] is to consider a flavour singlet quantity $X_s(m_u^{\text{rgi}}, m_d^{\text{rgi}}, m_s^{\text{rgi}})$ for example $X_\pi^2 = (2M_K^2 + M_\pi^2)/3$, $X_{t_0}^2 = 1/t_0$,

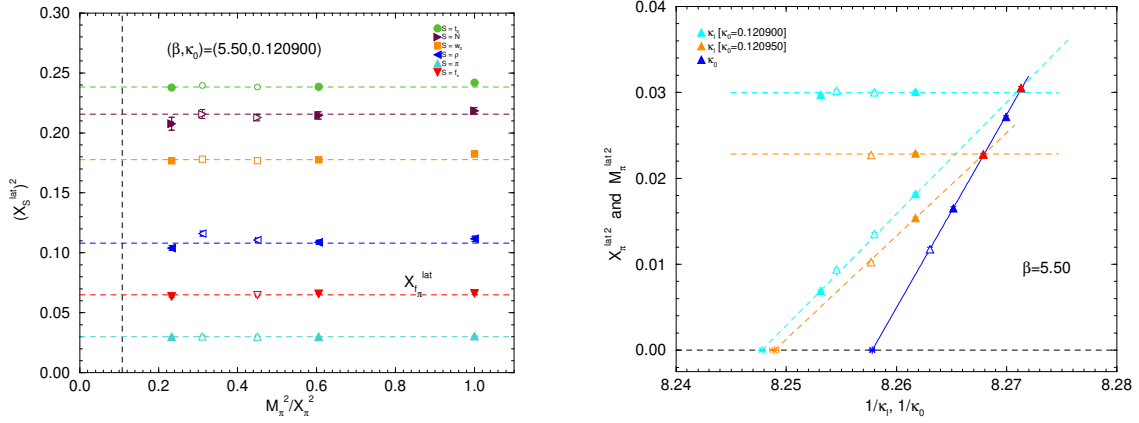


Figure 1: Left panel: $X_s^{\text{lat } 2}$ for $s = t_0, N, w_0, \rho, \pi, f_\pi$, for $(\beta, \kappa_0) = (5.50, 0.120900)$, together with constant fits. The opaque points have $M_\pi L \lesssim 4$ and are not considered in the fit. The vertical line is approximately the physical mass ratio value. The plot is taken from [6], to which we refer to for further details. Right panel: $X_\pi^{\text{lat } 2}$ along the $SU(3)$ -flavour symmetric line, blue triangles (with a linear fit) and along $a\bar{m} = \text{const.}$ lines starting from $\kappa_0 = 0.120900$, cyan horizontal triangles and $\kappa_0 = 0.120950$, orange horizontal triangles (both together with a constant fit). Also shown are the $M_\pi^{\text{lat } 2}$ lines for constant $\kappa_0 = 0.120900$, $\kappa_0 = 0.120950$ and varying $\kappa_u = \kappa_s \equiv \kappa_l$, cyan and orange triangles (both with a linear fit).

$X_N^2 = (M_N^2 + M_\Sigma^2 + M_\Xi^2)/3$. These are invariant under all u, d, s quark interchanges (by definition) and have the useful property that they have a stationary point on the $SU(3)$ -flavour symmetric line when all the quark masses are equal. This means that $X_s(\bar{m}^{\text{rgi}} + \delta m_u^{\text{rgi}}, \bar{m}^{\text{rgi}} + \delta m_d^{\text{rgi}}, \bar{m}^{\text{rgi}} + \delta m_s^{\text{rgi}}) = X_s(\bar{m}^{\text{rgi}}, \bar{m}^{\text{rgi}}, \bar{m}^{\text{rgi}}) + O((\delta m_q^{\text{rgi}})^2)$ where δm_q^{rgi} is the ‘distance’ from the $SU(3)$ -flavour symmetric line, \bar{m}^{rgi} being held constant (otherwise additional terms arise) [5]. As from eq. (7) $\bar{m}^{\text{rgi}} \propto a\bar{m}$, this result is valid whether renormalised or lattice is being considered. This is shown in the LH panel of Fig. 1. We use an $O(a)$ non-pertubatively improved clover action, [7], with $\beta = 10/g_0^2 = 5.40, 5.50, 5.65, 5.80$ and 5.95 on a variety of lattice sizes ($24^3 \times 48$, $32^3 \times 64$ and $48^3 \times 96$) with $M_\pi L \gtrsim 4$. Little evidence of any quadratic term $O((\delta(am_l))^2)$ and any systematic effect is seen for any $X_s^{\text{lat } 2}$ down to the physical point, so to within our accuracy we shall take $X_s^{\text{lat } 2}$ to be constant along any $a\bar{m} = \text{const}$ line. The RH panel in Fig. 1 shows the ratio $X_\pi^{\text{lat } 2}$ for various κ_0 and κ_l values as described in the figure caption. We have

$$X_s^{\text{lat } 2}(g_0, \bar{m}^{\text{rgi}}) = a^2(g_0, \bar{m}^{\text{rgi}})X_s^2(\bar{m}^{\text{rgi}}), \quad (20)$$

(again setting $\bar{m}^{\text{rgi}} \propto a\bar{m}$ in a) and forming a ratio gives

$$\frac{X_\pi^{\text{lat } 2}}{X_{t_0}^{\text{lat } 2}} = \frac{X_\pi^2(\bar{m}^{\text{rgi}})}{X_{t_0}^2(\bar{m}^{\text{rgi}})} = \frac{X_\pi'^2(0)\bar{m}^{\text{rgi}} + \dots}{X_{t_0}^2(0) + \dots} = \frac{X_\pi'^2(0)}{X_{t_0}^2(0)}\bar{m}^{\text{rgi}} + \dots = \frac{X_\pi'^2(0)}{X_{t_0}^2(0)}u(g_0)a\bar{m} + \dots \quad (21)$$

The first equality shows that $X_\pi^{\text{lat } 2}/X_{t_0}^{\text{lat } 2}$ can be taken as a proxy for \bar{m}^{rgi} . The second (and third) equalities use PCAC while the last equality has used the previous relation between \bar{m}^{rgi} and $a\bar{m}$, eq. (7). (So, for example, determining the $1/\kappa_0$ gradient of the $SU(3)$ -flavour symmetric line could give an indication of $(X_\pi'^2(0)/X_{t_0}^2(0))u(g_0)$.) However, while the RG equations in section 2 were developed with $a\bar{m}$, the present long extrapolation in $1/\kappa_0$ necessary to find κ_{0c} means that it is difficult to determine $a\bar{m}$ and so from eq. (21) we shall use instead $X_\pi^{\text{lat } 2}/X_{t_0}^{\text{lat } 2}$.

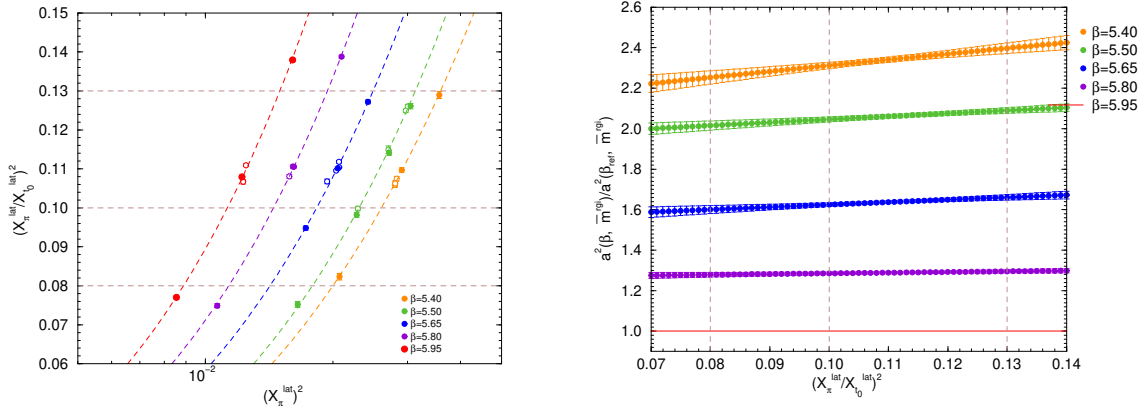


Figure 2: Left panel: $y = X_\pi^{\text{lat}2}/X_0^{\text{lat}2}$ versus $x = X_\pi^{\text{lat}2}$ (logarithmic scale) together with a 2-parameter fit $x = y(A + By)$ for our five β values. (the filled points lie on the $SU(3)$ -flavour symmetric lines, the opaque points are $a\bar{m} = \text{const.}$). Sample lines when the y -axis height $y_0 = 0.08, 0.10, 0.13$. Right panel: $a^2(\bar{m}^{\text{rgi}}, \beta)/a^2(\bar{m}^{\text{rgi}}, \beta_{\text{ref}})$ with $\beta_{\text{ref}} = 5.95$ versus $X_\pi^{\text{lat}2}/X_0^{\text{lat}2}$ for our five β values. The vertical lines correspond to the sample horizontal lines in the LH panel.

4. Lattice results

We now compare lattice spacings as a function of β with matching physics (i.e. same \bar{m}^{rgi}). So we plot for the y - and x -axes

$$y = \frac{X_\pi^{\text{lat}2}}{X_0^{\text{lat}2}} = \frac{X_\pi^2(\bar{m}^{\text{rgi}})}{X_0^2(\bar{m}^{\text{rgi}})}, \quad x = X_\pi^{\text{lat}2} = a^2(g_0, \bar{m}^{\text{rgi}})X_\pi^2(\bar{m}^{\text{rgi}}). \quad (22)$$

The y -axis is a proxy for the (physical) quark mass, \bar{m}^{rgi} . In the LH panel of Fig. 2 we show this plot, together with a 2-parameter fit $x = y(A + By)$, and with sample lines with the y -axis height $y_0 = 0.08, 0.10, 0.13$. The physical region is given by $y_0 \sim 0.09 - 0.10$.

If a depends only on β and negligibly on \bar{m}^{rgi} the lines will have the same slope at each point and be equidistant to each other. This can be illustrated by considering two β -values (β and β_{ref} say) with common \bar{m}^{rgi} (i.e. the same height for y -axis) then the ratio of the corresponding values on the x -axis is the ratio of lattice spacings only

$$\frac{x(\beta, \bar{m}^{\text{rgi}})}{x(\beta_{\text{ref}}, \bar{m}^{\text{rgi}})} = \frac{a^2(\beta, \bar{m}^{\text{rgi}})}{a^2(\beta_{\text{ref}}, \bar{m}^{\text{rgi}})}, \quad (23)$$

which when re-written as a difference: $\ln x(\beta, \bar{m}^{\text{rgi}}) - \ln x(\beta_{\text{ref}}, \bar{m}^{\text{rgi}}) = \ln(a^2(\beta, \bar{m}^{\text{rgi}})/a^2(\beta_{\text{ref}}, \bar{m}^{\text{rgi}}))$ should be approximately constant. This appears to be the case.

To check this in the RH panel of Fig. 2 we plot $a^2(\beta, \bar{m}^{\text{rgi}})/a^2(\beta_{\text{ref}}, \bar{m}^{\text{rgi}})$ with $\beta_{\text{ref}} = 5.95$ against $X_\pi^{\text{lat}2}/X_0^{\text{lat}2}$ and thus for many \bar{m}^{rgi} values¹. If there was no \bar{m}^{rgi} dependence these would be constant. Only for the coarsest lattice ($\beta = 5.40$) is there an appreciable deviation from constant behaviour, and this is small. For example in the figure range a 10% change in $X_\pi^2(\bar{m}^{\text{rgi}})/X_0^2(\bar{m}^{\text{rgi}})$ gives $\sim 1\text{-}2\%$ change in $a^2(5.40, \bar{m}^{\text{rgi}})/a^2(\beta_{\text{ref}}, \bar{m}^{\text{rgi}})$. So effectively there is only an overall shift in scale if we slightly miss a chosen value of the quark mass, \bar{m}^{rgi} .

¹The errors are estimated by considering fits $x = y(A + B(y - y_0))$ and varying y_0 . The error in A gives us the error in x at $y = y_0$, then used in eq. (23).

5. Lattice scaling

As the lattice spacing data is well described by linear behaviour in the quark mass, we can apply the formalism developed in the previous sections to investigate the scaling behaviour. From eq. (12) we can form $a^2(\beta, \bar{m}^{\text{rgi}})/a^2(\beta_{\text{ref}}, \bar{m}^{\text{rgi}})$. This gives

$$\frac{a^2(\beta, \bar{m}^{\text{rgi}})}{a^2(\beta_{\text{ref}}, \bar{m}^{\text{rgi}})} = \frac{s^2(\beta)}{s^2(\beta_{\text{ref}})} \left\{ 1 + D_{\pi/t_0}(\beta, \beta_{\text{ref}}) \frac{X_{\pi}^2(\bar{m}^{\text{rgi}})}{X_{t_0}^2(\bar{m}^{\text{rgi}})} \right\}. \quad (24)$$

with

$$D_{\pi/t_0}(\beta, \beta_{\text{ref}}) = 2 \left(\frac{r(\beta)}{u(\beta)} - \frac{r(\beta_{\text{ref}})}{u(\beta_{\text{ref}})} \right) \frac{X_{t_0}^2(0)}{X_{\pi}^2(0)}. \quad (25)$$

From our previous fits (LH panel of Fig. 2 and the associated fit parameters A, B) we can determine $s^2(\beta)/s^2(\beta_{\text{ref}})$ and the coefficient of $X_{\pi}^2(\bar{m}^{\text{rgi}})/X_{t_0}^2(\bar{m}^{\text{rgi}})$.

First recalling the solution for $s(g_0)$, eq. (14), we have

$$\frac{s^2(g_0)}{s^2(g_{0\text{ref}})} = \exp \left[-2 \int_{g_{0\text{ref}}}^{g_0} \frac{d\xi}{B_0(\xi)} \right]. \quad (26)$$

Guided by the knowledge of the β -function as given in eq. (5) we use the simplest $[2/2]$ Padé approximation as a fit function

$$B_0(g_0) = -\beta_{[2/2]}(g_0) = b_0 g_0^3 \frac{1 + \left(\frac{b_1}{b_0} - \frac{b_2^{\text{eff}}}{b_1} \right) g_0^2}{1 - \frac{b_2^{\text{eff}}}{b_1} g_0^2}. \quad (27)$$

(Note that eq. (26) can be integrated analytically.) Secondly we have

$$D_{\pi/t_0}(\beta, \beta_{\text{ref}}) = 2 \frac{X_{t_0}^2(0)}{X_{\pi}^2(0)} \int_{g_{0\text{ref}}}^{g_0} d\xi \frac{B_1(\xi)}{B_0^2(\xi) u(\xi)} \underbrace{\propto}_{g_0^2 \rightarrow 0} \int_{1/(2b_0 g_{0\text{ref}}^2)}^{1/(2b_0 g_0^2)} d\xi \xi^a e^{-\xi}, \quad (28)$$

where the LO result ($g_0^2 \rightarrow 0$) is given by the last expression with $a = (b_1 + b_0 d_0)/(2b_0^2)$ and can be written as the difference of incomplete- Γ functions. Numerically in our region of interest it is almost linear in β : i.e. $\propto \beta_{\text{ref}} - \beta$.

In the LH panel of Fig. 3 we show $s^2(\beta)/s^2(\beta_{\text{ref}})$ as blue points (from the previous fit), together with a further fit using eqs. (26), (27). Also shown is the two-loop β -function result (i.e. setting $b_2^{\text{eff}} = 0$ in eq. (27)) as an orange dashed line. $s^2(\beta)/s^2(\beta_{\text{ref}})$ is small, although growing at $\beta = 5.40$, it is still only about $\sim 10\%$. The RH panel of Fig. 3 shows $D_{\pi/t_0}(\beta, \beta_{\text{ref}})$ together with a fit as suggested by eq. (28) (with a one parameter fit for the proportionality constant).

Finally we wish to re-construct $a^2(\beta, \bar{m}^{\text{rgi}*})/a^2(\beta, \bar{m}^{\text{rgi}*})$, via eq. (24), with the fit function results as shown in Fig. 3. In Fig. 4 we plot $a^2(\beta, \bar{m}^{\text{rgi}*})/a^2(\beta_{\text{ref}}, \bar{m}^{\text{rgi}*})$ against β from eq. (24), using values of $X_{\pi}^2(\bar{m}^{\text{rgi}*})/X_{t_0}^2(\bar{m}^{\text{rgi}*}) = 0.099(3)$, QCDSF15 [8]² and as a comparison 0.091(1), FLAG24 [9]. As expected from our previous results (as exemplified by Fig. 2) there is little numerical difference between the two values of $\bar{m}^{\text{rgi}*}$. Comparing the results using this RG-guided approach with each value being found separately (the magenta points), we have achieved a smoother behaviour for the lattice spacing.

²The $\beta = 5.95$ result was determined later, using the methods described in [8] as 0.0521(4) fm.

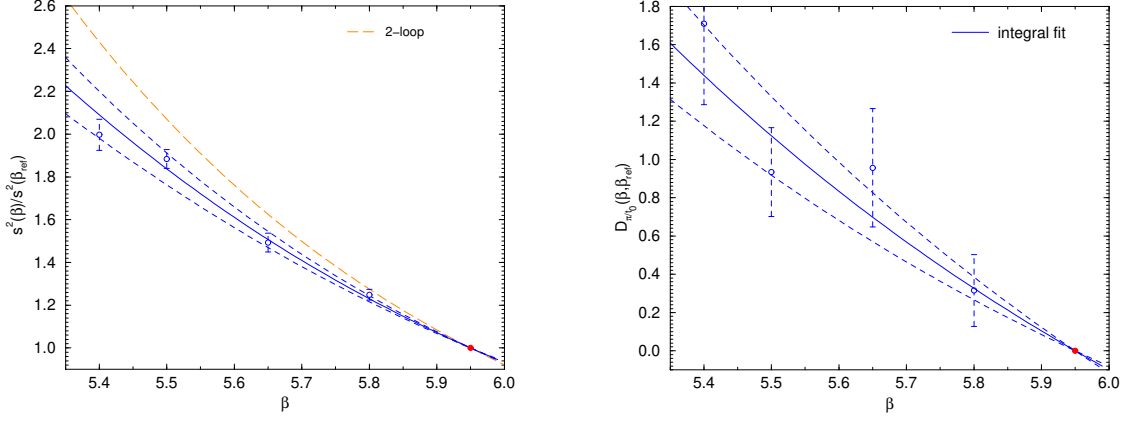


Figure 3: Preliminary results. Left panel: $s^2(\beta)/s^2(\beta_{\text{ref}})$ versus β ($\beta_{\text{ref}} = 5.95$) blue line from the fit results given by the ratios from eq. (26) (with eq. (27)) as the blue points. The orange dashed line is the result from the two-loop β -function ($b_2^{\text{eff}} = 0$). Right panel: $D_{\pi/t_0}(\beta, \beta_{\text{ref}})$ versus β , with the fit as indicated in eq. (28).

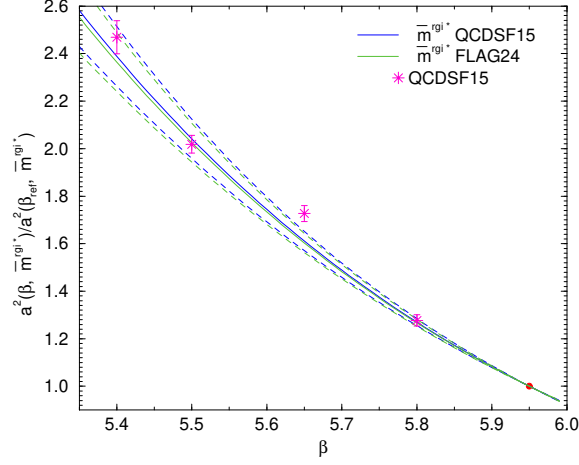


Figure 4: Preliminary results. $a^2(\beta, \bar{m}^{\text{rgi}*})/a^2(\beta_{\text{ref}}, \bar{m}^{\text{rgi}*})$ against β ($\beta_{\text{ref}} = 5.95$), using our previous determination of $X_{\pi}^2(\bar{m}^{\text{rgi}*})/X_{t_0}^2(\bar{m}^{\text{rgi}*})$, QCDSF15 [8], as a blue line. Also shown are the results arising from FLAG24 [9] for $X_{\pi}^2(\bar{m}^{\text{rgi}*})/X_{t_0}^2(\bar{m}^{\text{rgi}*})$, green line. Furthermore as a comparison we show our previous results, QCDSF15, as magenta stars.

6. Conclusions

In this talk we have discussed RG equations for 2+1 clover fermions and attempted to construct some RG functions. Considering the lattice spacing, we find scaling, with little dependence on $\bar{m}^{\text{rgi}*}$. The next steps, [1], could be to reduce the errors on the lattice spacing ratios with more $SU(3)$ -flavour symmetric data, using a more sophisticated fit procedure and to determine $\bar{m}^{\text{rgi}*}$ accurately at one value of β_{ref} and hence a value of a fm, using (e.g.) the nucleon baryon octet, [8]. A possible advantage of the method is that lattice spacing ratios can be more precisely determined at many β values (using e.g. as here, accurate pion mass and gradient flow data). The general possibility is that this might lead to smoother continuum extrapolations.

Acknowledgments

The numerical configuration generation (using the BQCD lattice QCD program [10]) and data analysis (using the CHROMA software library [11]) was carried out on the DiRAC Blue Gene Q and Extreme Scaling Service (Edinburgh Centre for Parallel Computing (EPCC), Edinburgh, UK), the Data Intensive Service (Cambridge Service for Data-Driven Discovery, CSD3, Cambridge, UK), the Gauss Centre for Supercomputing (GCS) supercomputers JUQUEEN and JUWELS (John von Neumann Institute for Computing, NIC, Jülich, Germany) and resources provided by the North-German Supercomputer Alliance (HLRN), the National Computer Infrastructure (NCI National Facility in Canberra, Australia supported by the Australian Commonwealth Government) and the Phoenix HPC service (University of Adelaide). K.U.C. is supported by the ARC Grant No. DP220103098. R.H. is supported in part by the STFC Grant No. ST/X000494/1. P.E.L.R. is supported in part by the STFC Grant No. ST/G00062X/1. G.S. is supported by DFG Grant No. SCHI 179/8-1. R.D.Y. and J.M.Z. are supported by the ARC Grants No. DP220103098 and DP240102839. For the purpose of open access, the authors have applied a Creative Commons Attribution (CC BY) licence to any author accepted manuscript version arising from this submission.

References

- [1] QCDSF Collaboration, in preparation.
- [2] M. Lüscher *et al.*, *Nucl. Phys. B* **478** (1996) 365, [[arXiv:hep-lat/9605038 \[hep-lat\]](#)].
- [3] S. Sint *et al.*, *Nucl. Phys. B* **465** (1996) 71, [[arXiv:hep-lat/9508012 \[hep-lat\]](#)].
- [4] M. Dalla Brida *et al.*, *JHEP* **2024** (2024) 188, [[arXiv:2401.00216 \[hep-lat\]](#)].
- [5] W. Bietenholz *et al.*, *Phys. Rev. D* **84** (2011) 054509, [[arXiv:1102.5300 \[hep-lat\]](#)].
- [6] V. G. Bornyakov *et al.*, *Phys. Lett. B* **767** (2017) 366, [[arXiv:1612.04798 \[hep-lat\]](#)].
- [7] N. Cundy *et al.*, *Phys. Rev. D* **79** (2009) 094507, [[arXiv:0901.3302 \[hep-lat\]](#)].
- [8] V. G. Bornyakov *et al.*, [[arXiv:1508.05916 \[hep-lat\]](#)].
- [9] Y. Aoki *et al.*, [Flavour Lattice Averaging Group (FLAG)], [[arXiv:2411.04268 \[hep-lat\]](#)].
- [10] T. R. Haar *et al.*, *EPJ Web Conf.* **175** (2018) 14011, [[arXiv:1711.03836 \[hep-lat\]](#)].
- [11] R. G. Edwards *et al.*, *Nucl. Phys. B Proc. Suppl.* **140** (2005) 832, [[arXiv:hep-lat/0409003](#)].